Electronic Supplementary Material (ESI) for Inorganic Chemistry Frontiers.

Electronic Supporting Information

Heterovalent Chalcogen Bonding. Supramolecular Assembly Driven by the Occurrence of the Tellurium(II)···Ch(I) (Ch = S, Se, Te) Linkage

Yury V. Torubaev [a,b]*, Anton V. Rozhkov [c], Ivan V. Skabitsky [a], Rosa M. Gomila[d], Antonio Frontera[d], Vadim Yu. Kukushkin [c,e]*

---

a. N. S. Kurnakov Institute of General and Inorganic Chemistry, of Russian Academy of Sciences, Moscow, 119991 Russian Federation. E-mail: torubaev@igic.ras.ru
b. Department of Molecular Chemistry and Materials Science, Weizmann Institute of Science, Rehovot 7610001, Israel
c. Institute of Chemistry, Saint Petersburg State University, Universitetskaya Nab. 7/9, Saint Petersburg, 199034 Russian Federation. E-mail: v.kukushkin@spbu.ru
d. Department of Chemistry, Universitat de les Illes Balears, 07122 Palma de Mallorca, Baleares, Spain. E-mail: toni.frontera@uib.es
e. Institute of Chemistry and Pharmaceutical Technologies, Altai State University, 656049 Barnaul, Russian Federation

Contents

Crystal data and structure refinement

Table S1. Crystal data and structure refinement for **1**–**4**.

Identification code	**1**	**2**	**3**	**4**
Empirical formula	$C_{26}H_{10}F_{14}S_2Te$	$C_{26}H_{10}F_{14}Se_2Te$	$C_{26}H_{10}F_{14}Te_3$	$C_{22}H_{10}F_8N_2Se_2Te$
Formula weight	780.06	873.86	971.14	739.84
Temperature, K	100(2)	100(2)	100(2)	100(2)
Crystal size, mm	0.07 × 0.02 × 0.01	0.3 × 0.1 × 0.1	0.49 × 0.38 × 0.27	0.1 × 0.1 × 0.06
Wavelength, Å	1.54184	0.71073	0.71073	1.54184
Crystal system	orthorhombic	triclinic	monoclinic	triclinic
Space group	$Pna2_1$	P-1	P2/n	P-1
a, Å	27.4374(4)	5.8848(3)	20.3887(10)	5.8234(2)
b, Å	17.3113(2)	14.7941(8)	6.3639(3)	14.1653(3)
c, Å	5.48880(10)	15.6028(9)	21.1622(9)	15.1819(4)
α, deg.	90	92.780(2)	90	66.908(2)
β, deg.	90	93.866(2)	93.483(2)	84.933(2)
γ, deg.	90	96.426(2)	90	84.565(2)
V, Å^3	2607.05(7)	1344.62(13)	2740.8(2)	1145.04(6)
Z	4	2	4	2
Density (calc.), g/cm^3	1.987	2.158	2.354	2.146
μ, mm^{-1}	11.623	3.928	3.285	14.640
F(000)	1504.0	824.0	1792.0	696.0
2Θ range for data	6.036 to 144.992	3.922 to 57.99	5.388 to 59.994	6.338 to 152.822

collection, deg.				
Index ranges	-33 ≤ h ≤ 33, -20 ≤ k ≤ 21, -6 ≤ l ≤ 6	-8 ≤ h ≤ 8, -20 ≤ k ≤ 20, -21 ≤ l ≤ 21	-28 ≤ h ≤ 28, -8 ≤ k ≤ 8, -29 ≤ l ≤ 29	-7 ≤ h ≤ 7, -17 ≤ k ≤ 17, -17 ≤ l ≤ 19
Reflections collected	37253	20900	49700	18274
Independent reflections	5129 [R_{int}= 0.1278, R_{sigma}= 0.0568]	7113 [R_{int}= 0.0874, R_{sigma}= 0.1200]	7968 [R_{int} = 0.0472, R_{sigma} = 0.0287]	4729 [R_{int} = 0.0485, R_{sigma} = 0.0330]
R_1 / wR_2 ($I > 2\sigma(I)$)	0.0710/0.1635	0.0458/0.0793	0.0214/0.0462	0.0300/0.0763
R_1 / wR_2 (all data)	0.0751/0.1650	0.1074/0.0955	0.0247/0.0479	0.0306/0.0771
Goodness-of-fit on F^2	1.070	0.948	1.089	1.056
Largest diff. peak/hole, e Å^{-3}	0.89/-1.23	0.91/-0.77	0.67/-0.65	1.27/-1.10

The Cambridge Structural Database (CSD) search for heterovalent Ch···Te (Ch = S, Se, Te) contacts

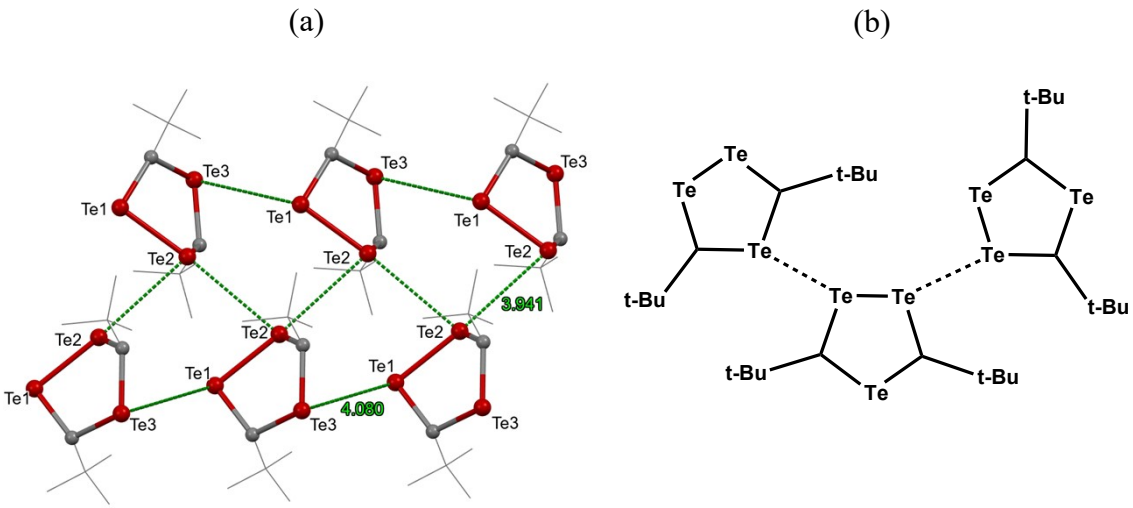

Figure S1. (a) A fragment of the crystal structure of $Te^{I}_{2}(CH^{t}Bu)_{2}Te^{II}$ (CSD refcode: COWQUB). The dotted lines denote significantly shortened contacts exhibiting distances smaller than R_{vdW}(Te)+R_{vdW}(Te). *tert*-Butyl groups are omitted for clarity; (b) Schematic representation of discussed contacts.

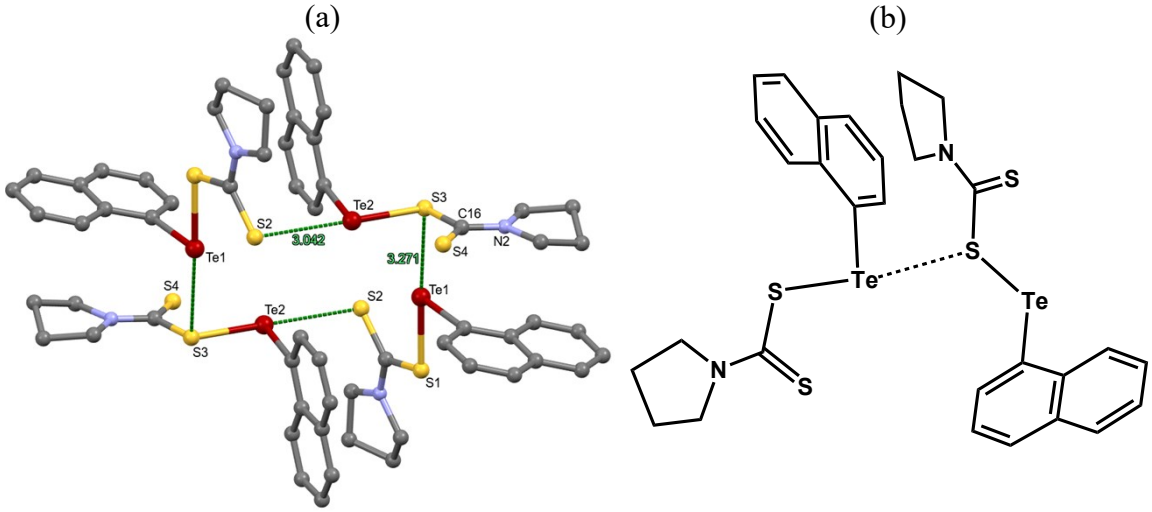

Figure S2. (a) A fragment of the crystal structure of dithiocarbamatopyrrolidine naphthyl tellurium (II) (CSD refcode: KOLTAH). The dotted lines denote significantly shortened contacts exhibiting distances smaller than R_{vdW}(Te)+R_{vdW}(Te). Hydrogen atoms are omitted for clarity; (b) Schematic representation of discussed contacts.

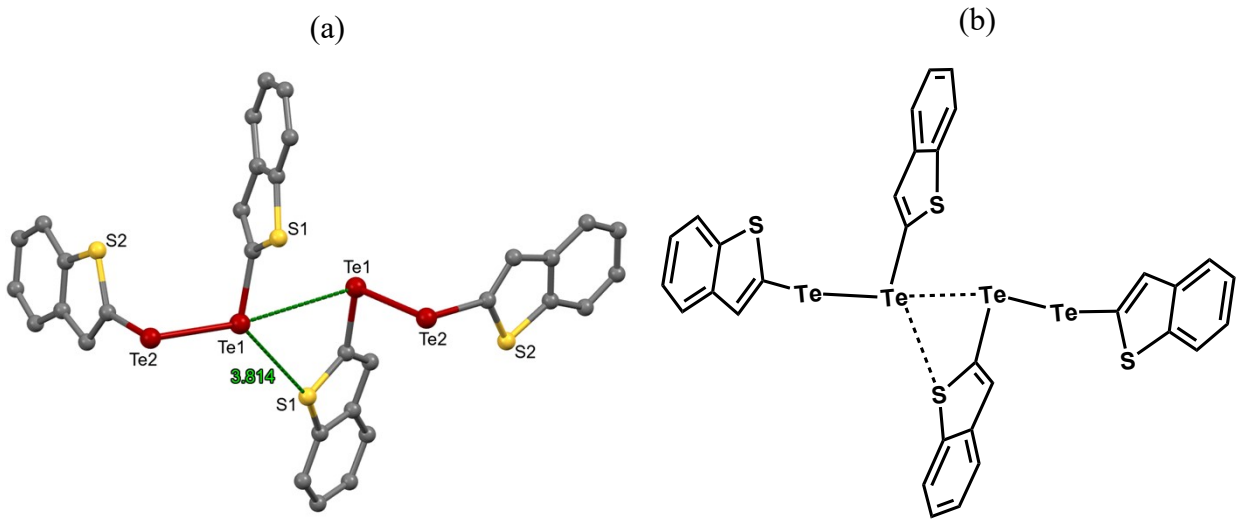

Figure S3. (a) A fragment of the crystal packing of bis(2-Benzo(b)thienyl)-di-tellurium (CSD refcode: VIBNEZ) (b) Schematic representation of discussed contacts.

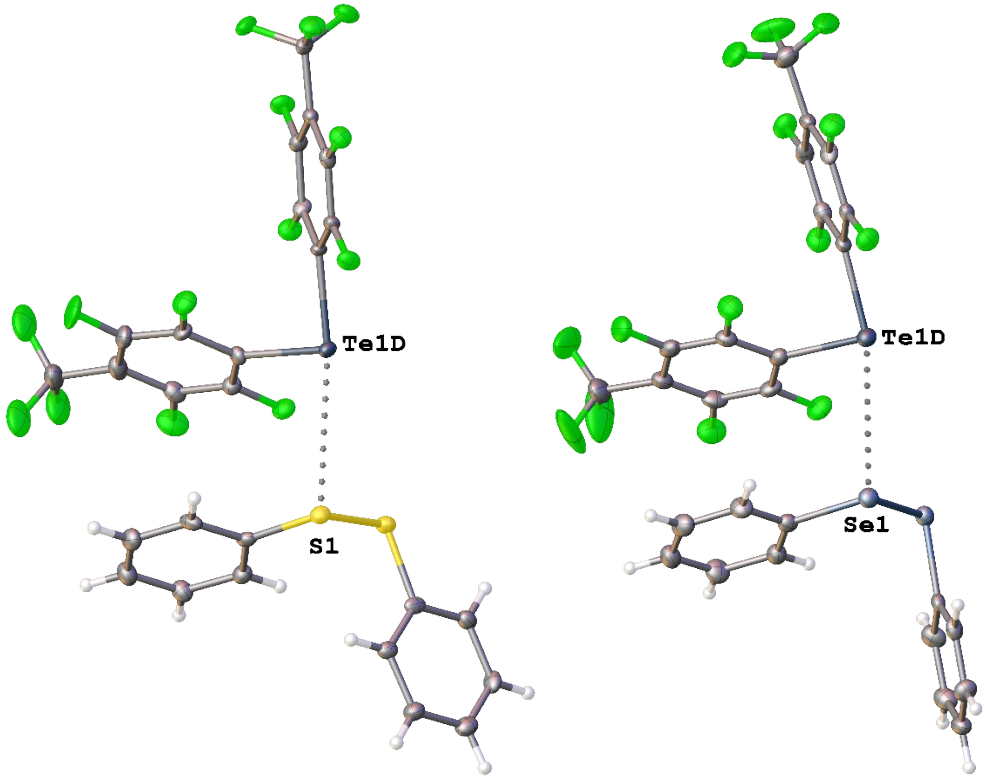

1 **2**

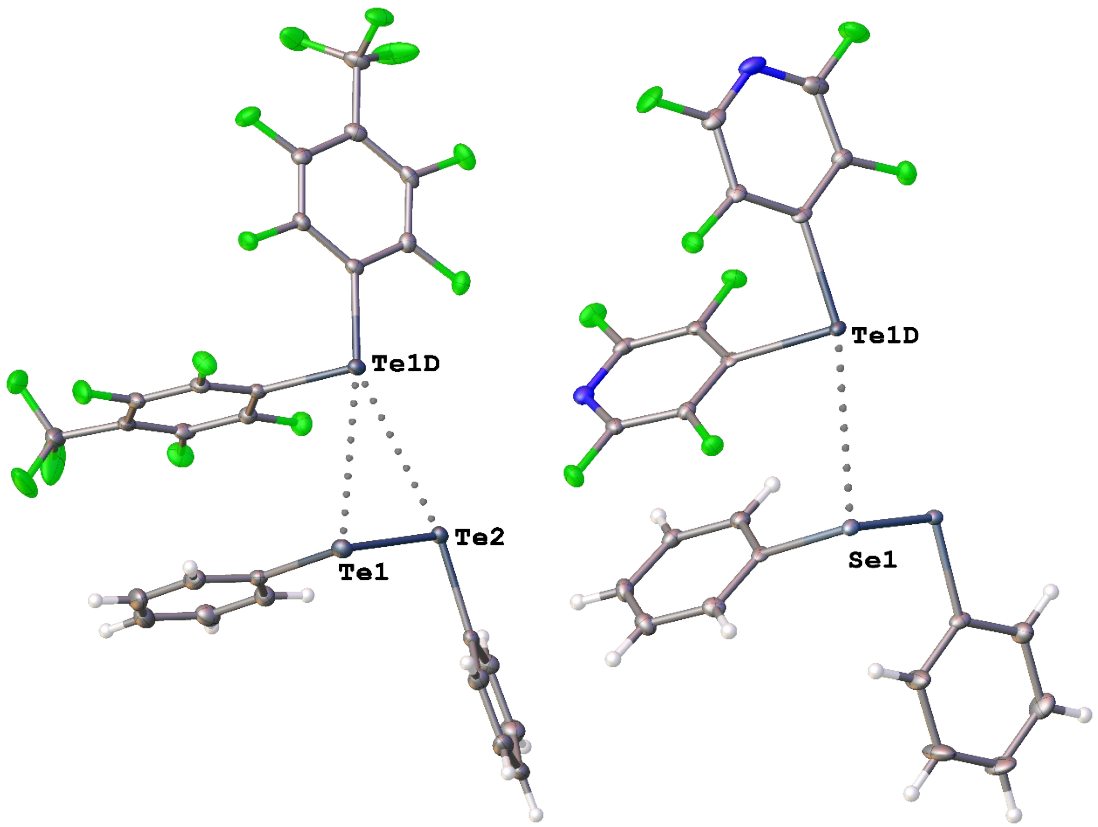

3 **4**

Figure S4. Geometry of the dimeric associates in **1**–**4**.

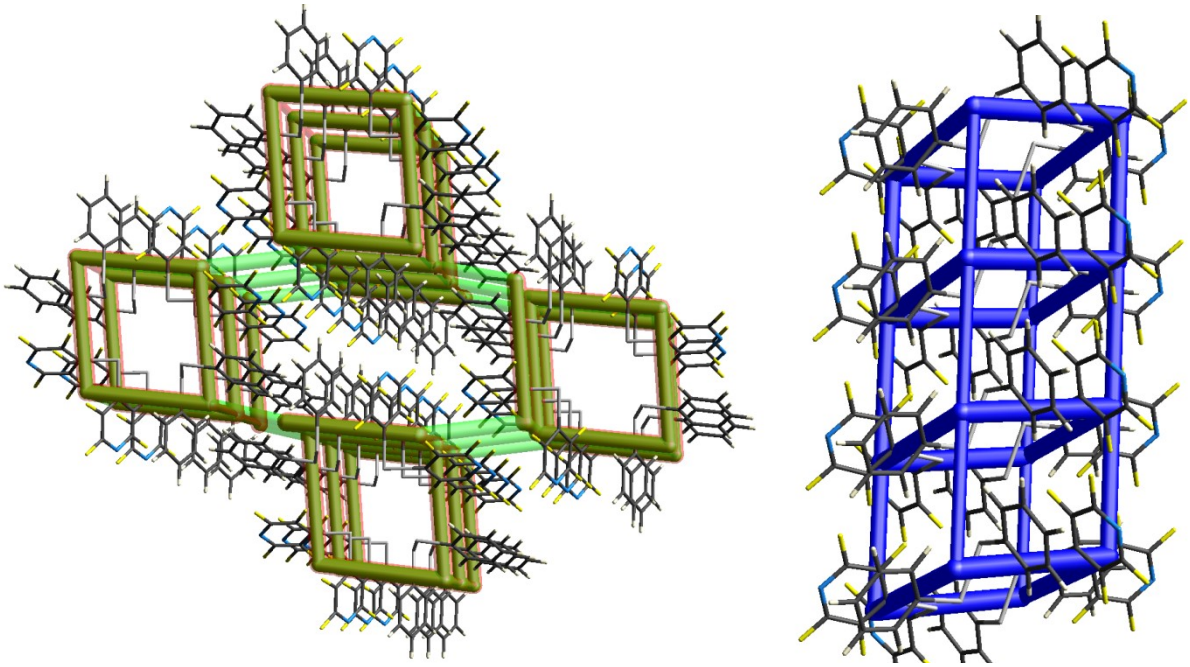

a **b**

Figure S5. A fragment of the energy framework for **4** (a, b). Electrostatic component of total intermolecular interaction energy is given in red, while its dispersion component in green; total intermolecular interaction energy is provided in blue.

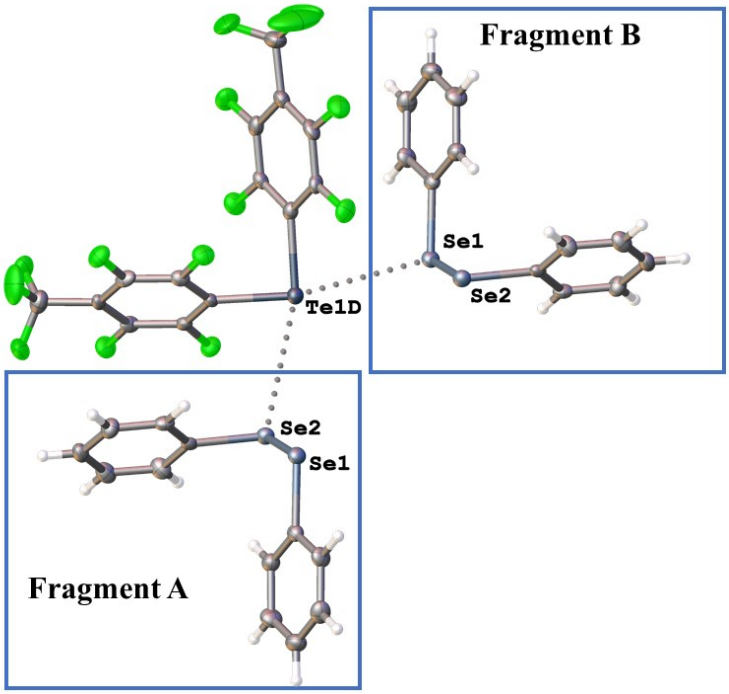

Figure S6. Fragments of **2**.

Computational details

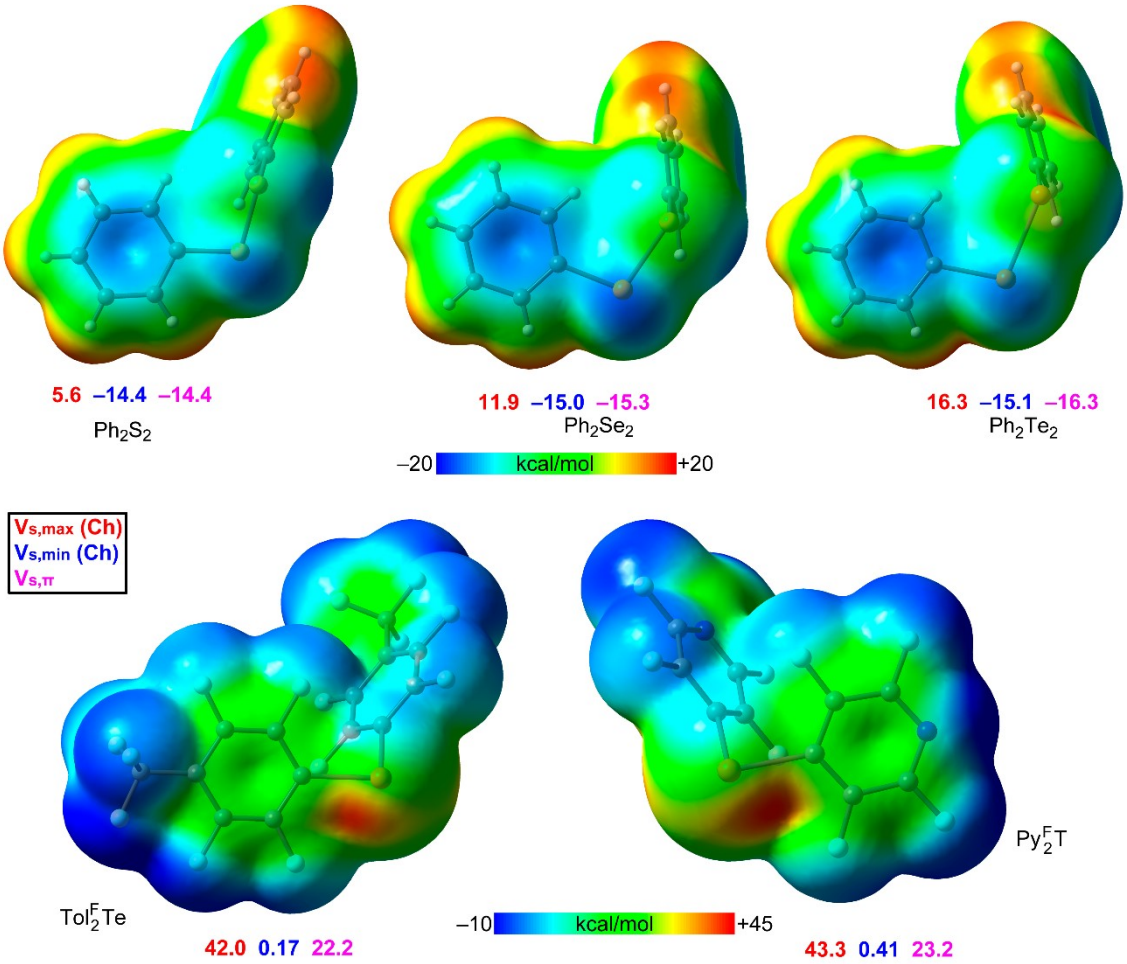

Figure S7. MEP surfaces of the Ch^{I} (a) and Ch^{II} (b) partners used in this work at the PBE0-D3/def2-TZVP. Values in red and blue correspond to maximum and minimum values at the Ch-atom. Values in fuchsia are measured over the center of the aromatic rings. Isovalue 0.001 a.u. Values in kcal/mol.

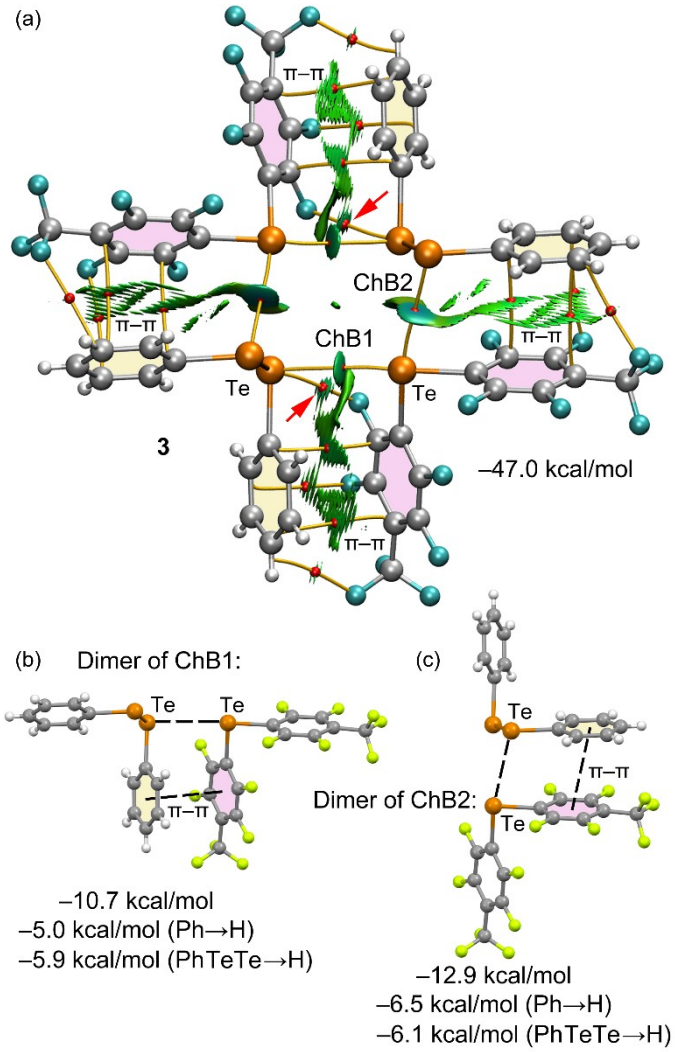

Figure S8. (a) Combined QTAIM (bond CPs in red and bond paths as orange lines) and NCIplot (RDG isosurface 0.45 a.u., $\rho_{cut\text{-}off}$ = 0.04 a.u., range $-0.035 \leq (sign\lambda_2)\rho \leq 0.035$ a.u.) analyses of the tetramer of **3**; (b,c) Two dimers extracted from the tetramer with indication of the interaction energies and those of their mutated dimers.

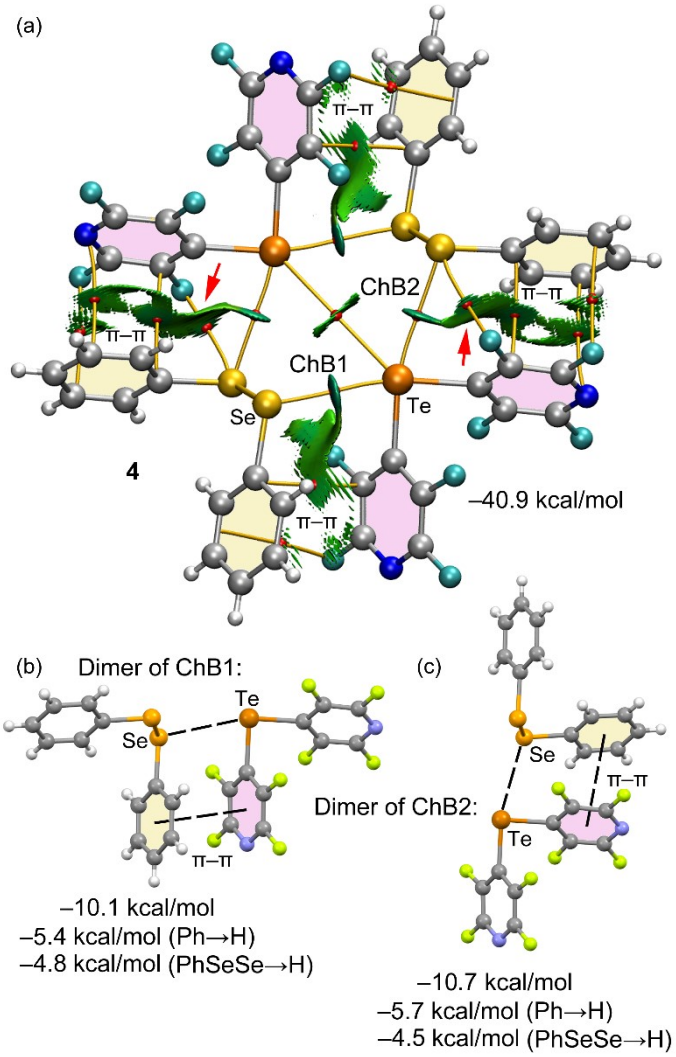

Figure S9. (a) Combined QTAIM (bond CPs in red and bond paths as orange lines) and NCIplot (RDG isosurface 0.45 a.u., $\rho_{cut\text{-}off}$ = 0.04 a.u., range $-0.035 \leq (sign\lambda_2)\rho \leq 0.035$ a.u.) analyses of the tetramer of **4**; (b,c) Two dimers extracted from the tetramer with indication of the interaction energies and those of their mutated dimers.

Table S2. QTAIM parameters (electron density, Lagrangian kinetic energy density, potental energy density and Laplacian of electron density, in a.u.) at the bond CPs characterizing the ChBs in compounds **1**–**4**. See Figure 2 (main text) for labelling of atoms.

CP	ρ	G_r	V_r	H_r	$\nabla^2\rho$
Compound **1**					
S1···Te1D	1.21E-02	6.27E-03	-5.50E-03	7.74E-04	2.82E-02
Compound **2**					
Se1···Te1D	1.36E-02	6.49E-03	-6.23E-03	2.67E-04	2.70E-02
Se2···Te1D	1.22E-02	5.86E-03	-5.45E-03	4.15E-04	2.51E-02
Te1D···Te1D	1.43E-03	6.90E-04	-4.29E-04	2.61E-04	3.81E-03
Compound **3**					
Te1···Te1D	1.03E-02	4.21E-03	-3.90E-03	3.04E-04	1.80E-02
Te2···Te1D	1.47E-02	6.20E-03	-6.31E-03	-1.03E-04	2.44E-02
F··Te2	9.15E-03	6.67E-03	-5.02E-03	1.65E-03	3.33E-02
Compound **4**					
Se1···Te1D	1.22E-02	5.81E-03	-5.42E-03	3.93E-04	2.48E-02
Se2···Te1D	1.44E-02	6.89E-03	-6.71E-03	1.85E-04	2.83E-02
F··Se2	6.64E-03	5.20E-03	-3.72E-03	1.49E-03	2.67E-02
Te1D···Te1D	1.74E-03	8.40E-04	-5.38E-04	3.02E-04	4.56E-03

Thermal properties of Ph_2Ch_2 (Ch = S, Se, Te) and adducts 1–4

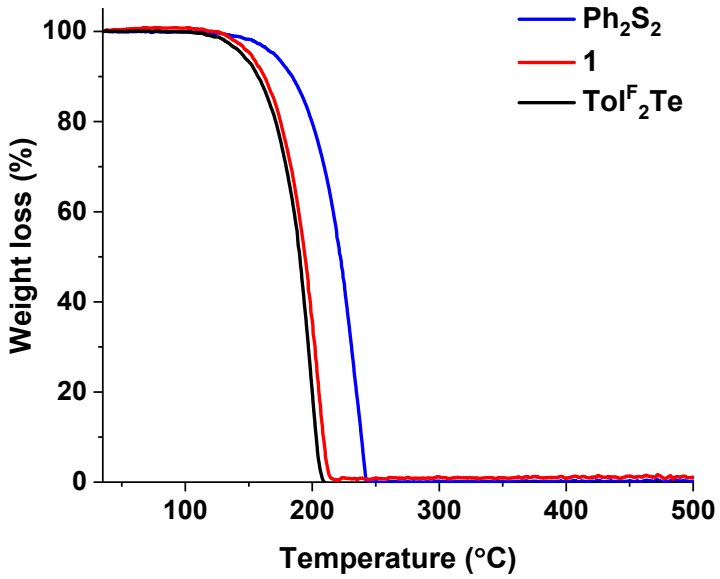

Figure S10. TGA curves of Ph_2S_2 (blue), **1** (red) and $Tol^F{}_2Te$ (black).

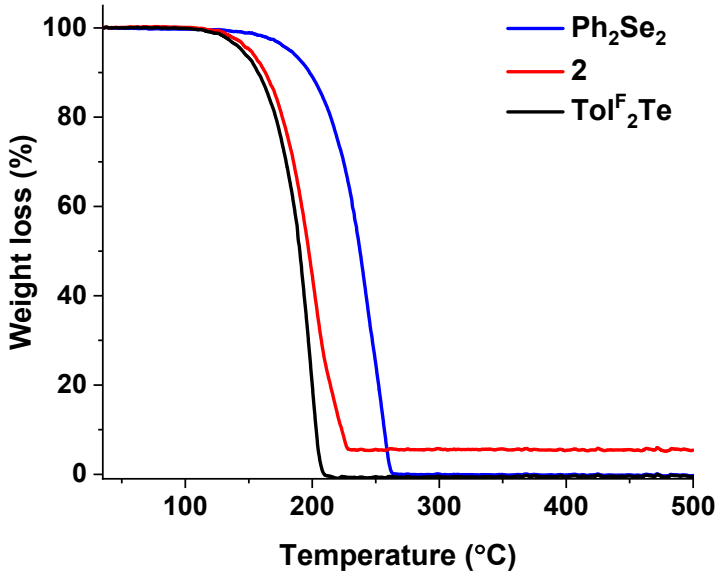

Figure S11. TGA curves of Ph_2Se_2 (blue), **2** (red) and $Tol^F{}_2Te$ (black).

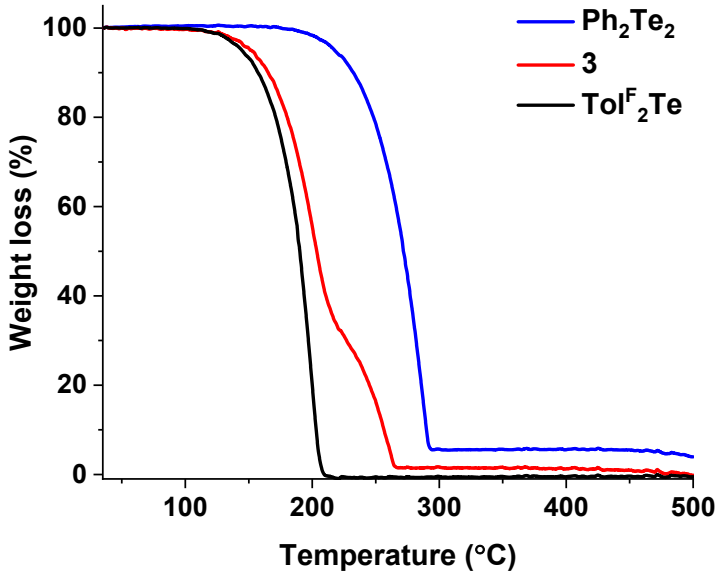

Figure S12. TGA curves of Ph_2Te_2 (black), **3** (red) and $Tol^F{}_2Te$ (black).

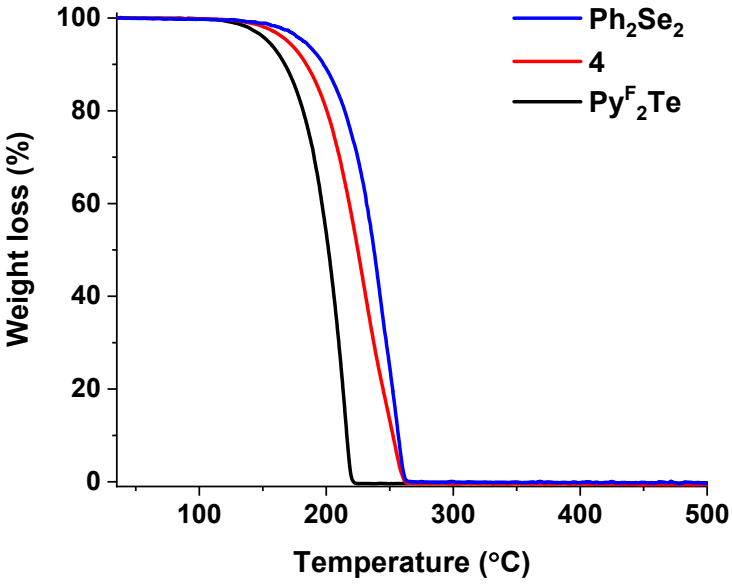

Figure S13. TGA curves of Ph_2Se_2 (blue), **4** (red) and $Py^F{}_2Te$ (black).

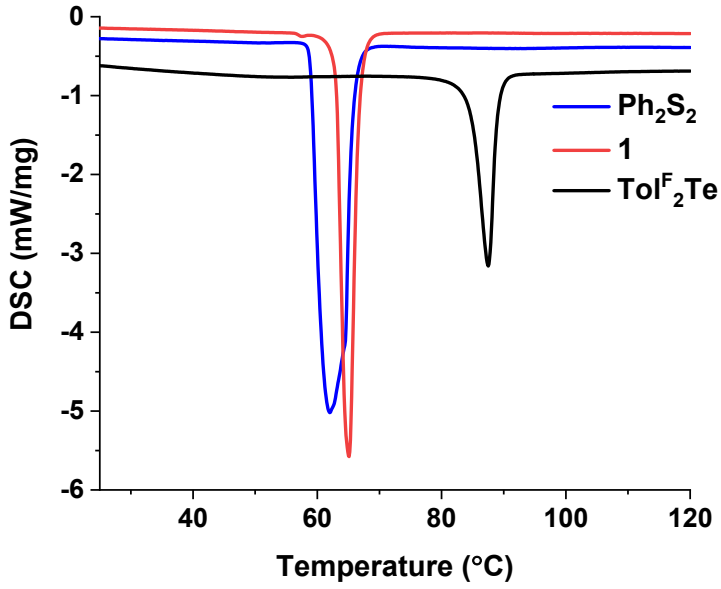

Figure S14. DSC curves of Ph_2S_2 (blue), **1** (red) and Tol^F_2Te (black).

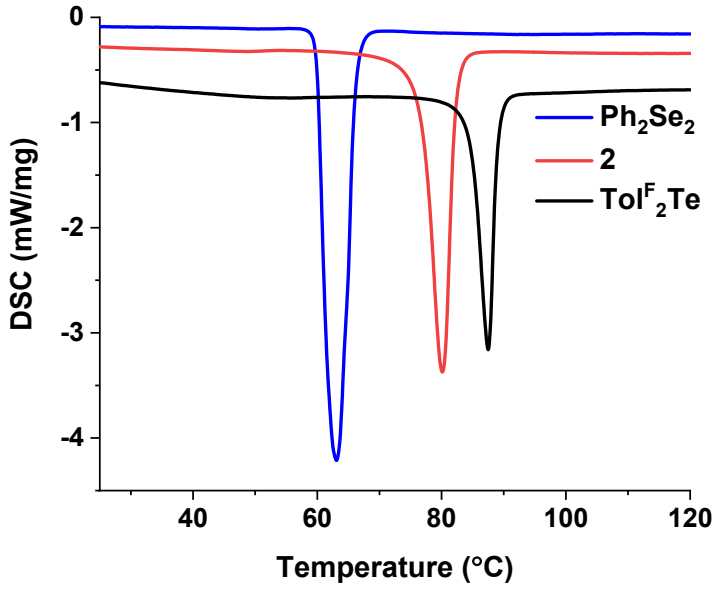

Figure S15. DSC curves of Ph_2Se_2 (blue), **2** (red) and Tol^F_2Te (black).

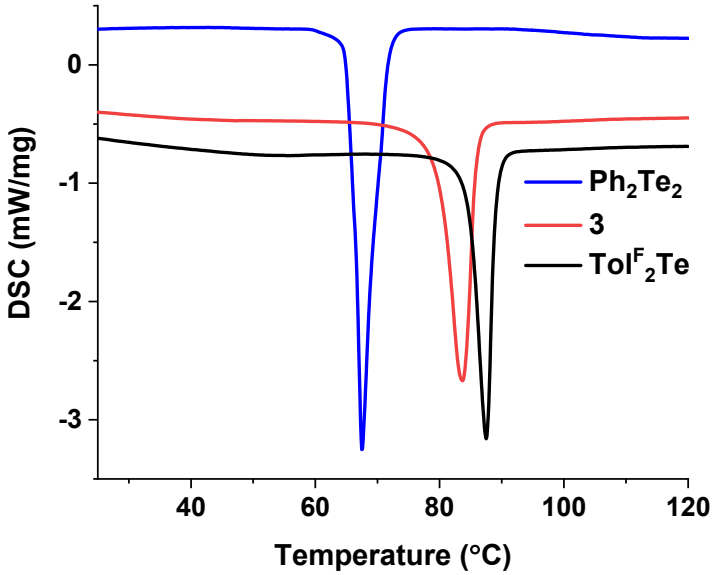

Figure S16. DSC curves of Ph_2Te_2 (blue), **3** (red) and $Tol^F{}_2Te$ (black).

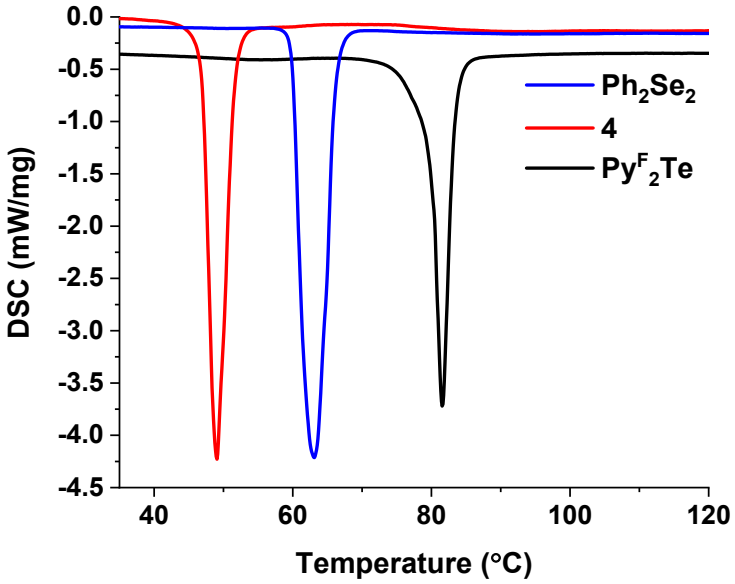

Figure S17. DSC curves of Ph_2Se_2 (blue), **4** (red) and $Py^F{}_2Te$ (black).

Table S3. Thermal properties of **1**–**4**.

Entry	mp, °C	T_d, °C*
Tol^F_2Te	88	144
Ph_2S_2	62	170
1	65	151
Ph_2Se_2	63	182
2	82	151
Ph_2Te_2	68	217
3	85	152
Py^F_2Te	82	154
4	49	169

* Related to 5% weight loss.

Heterovalent chalcogen bonding in solution

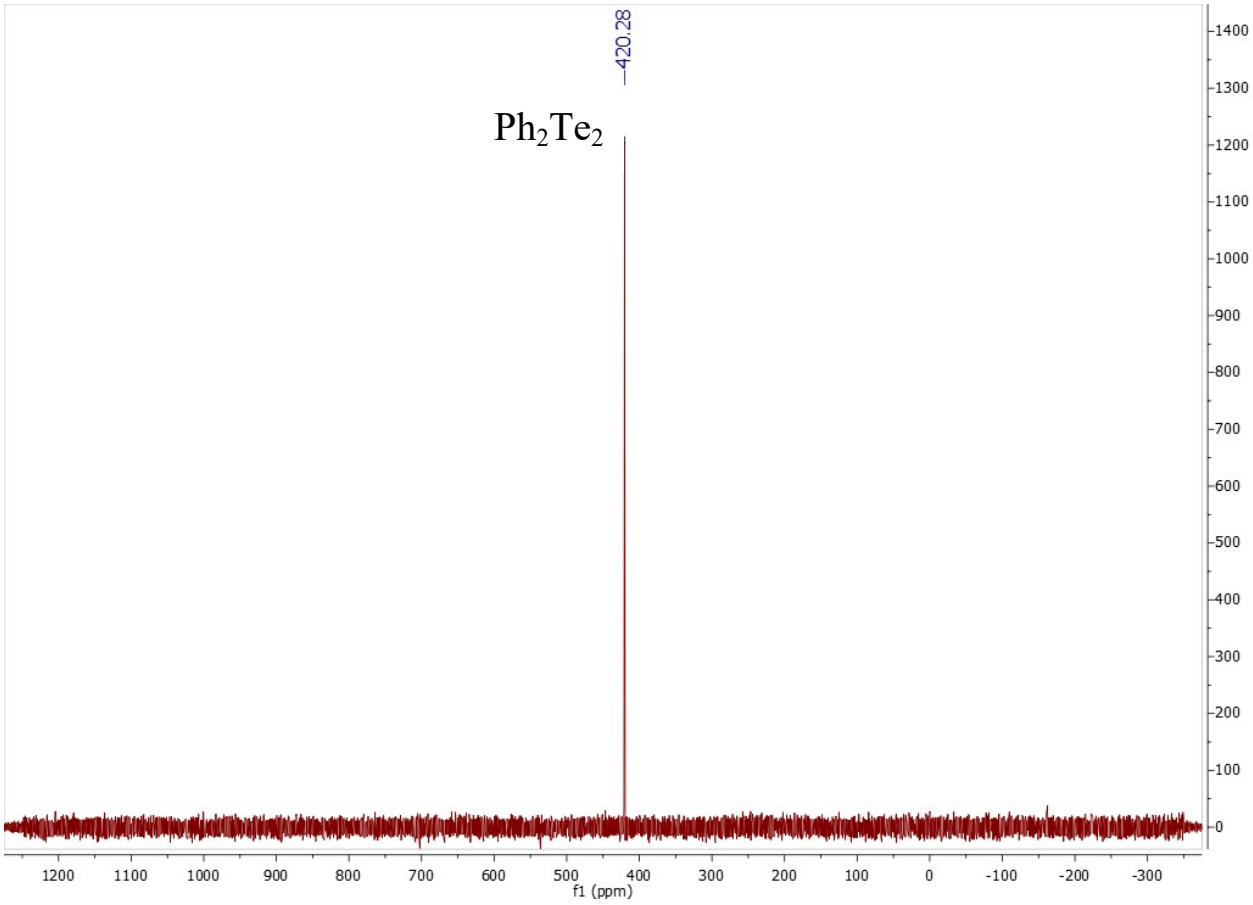

Figure S18. ^{125}Te NMR spectrum of Ph_2Te_2 in $CDCl_3$ at 298 K.

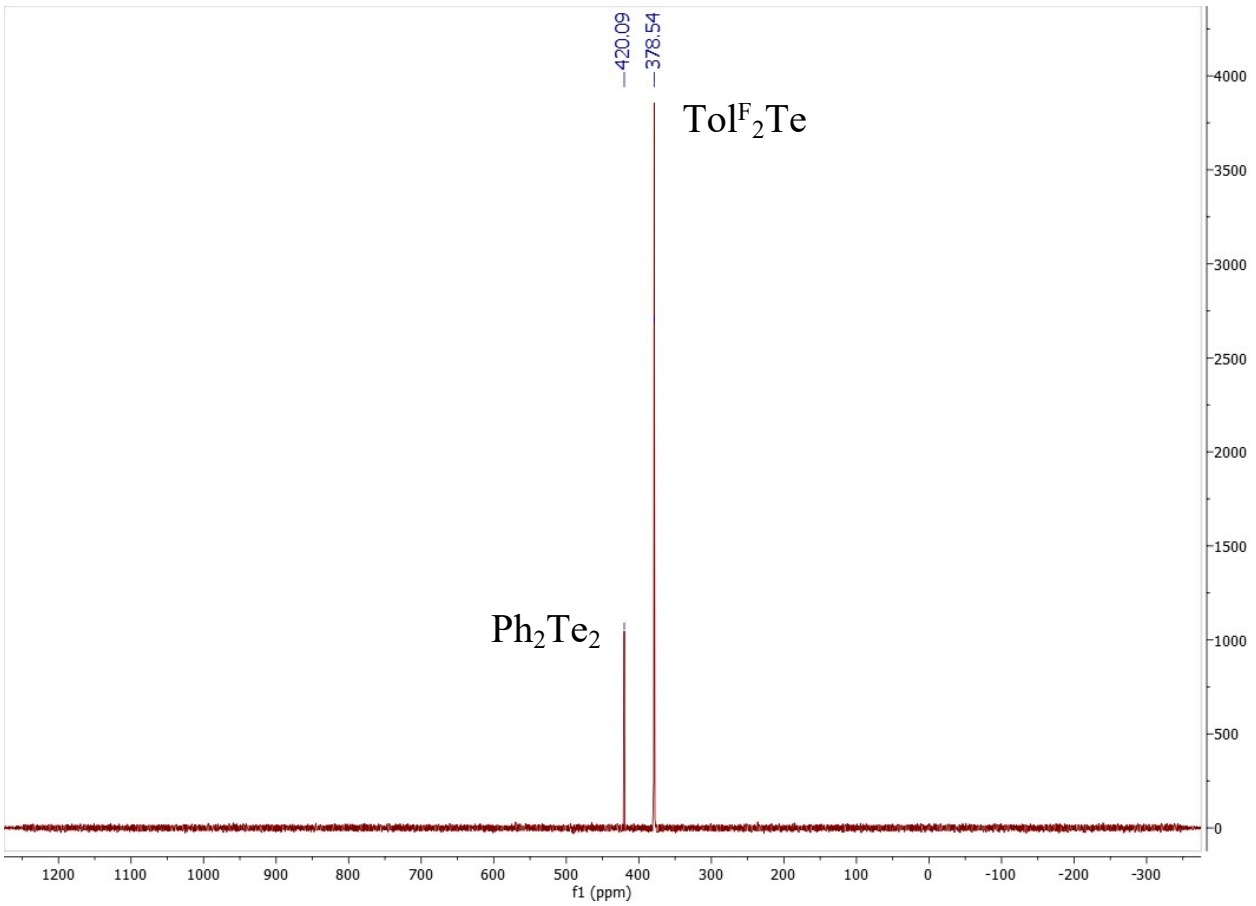

Figure S19. ^{125}Te NMR spectrum of mixture Tol$^F_2$Te:Ph$_2$Te$_2$ in molar ratio 20:1 in $CDCl_3$ at 298 K.

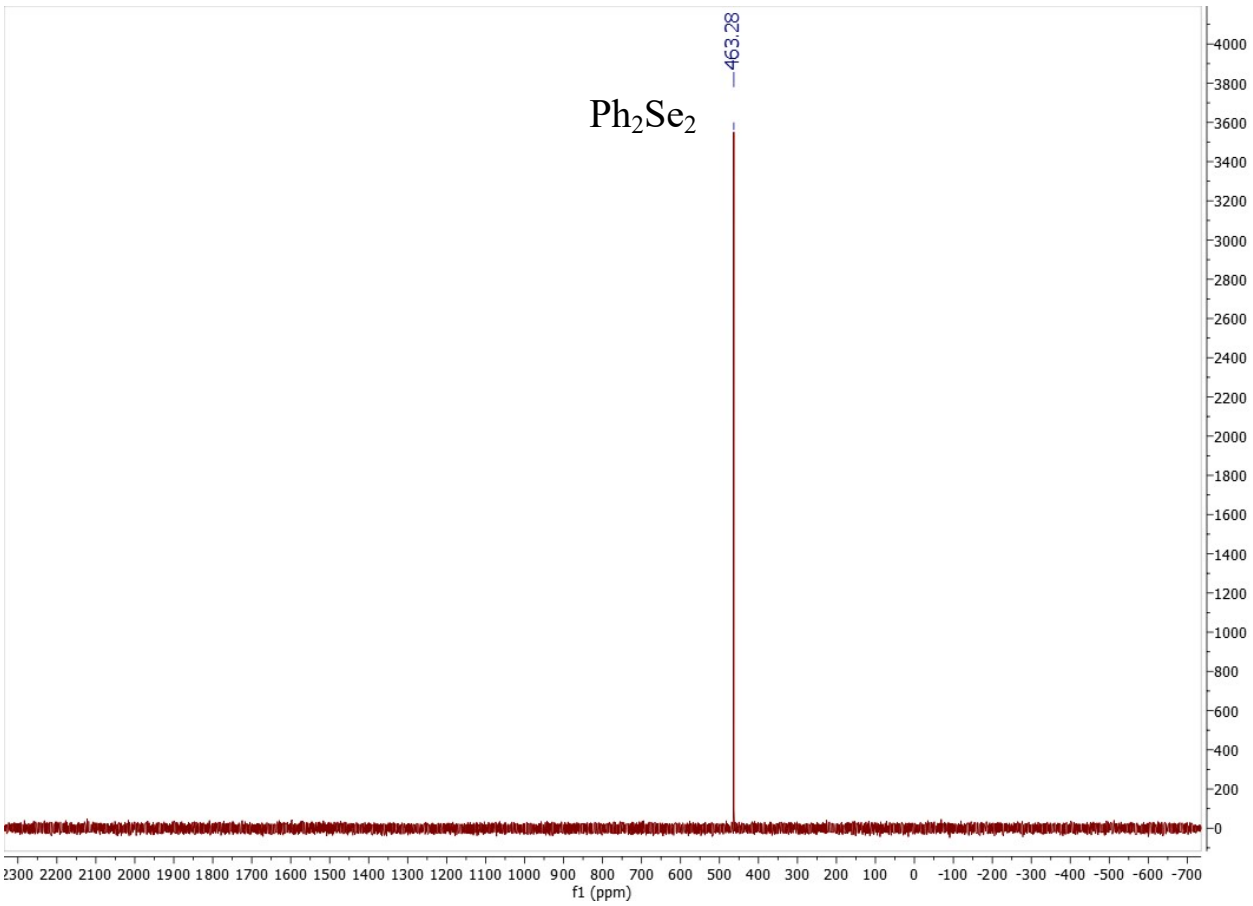

Figure S20. ^{77}Se NMR spectrum of Ph_2Se_2 in $CDCl_3$ at 298 K.

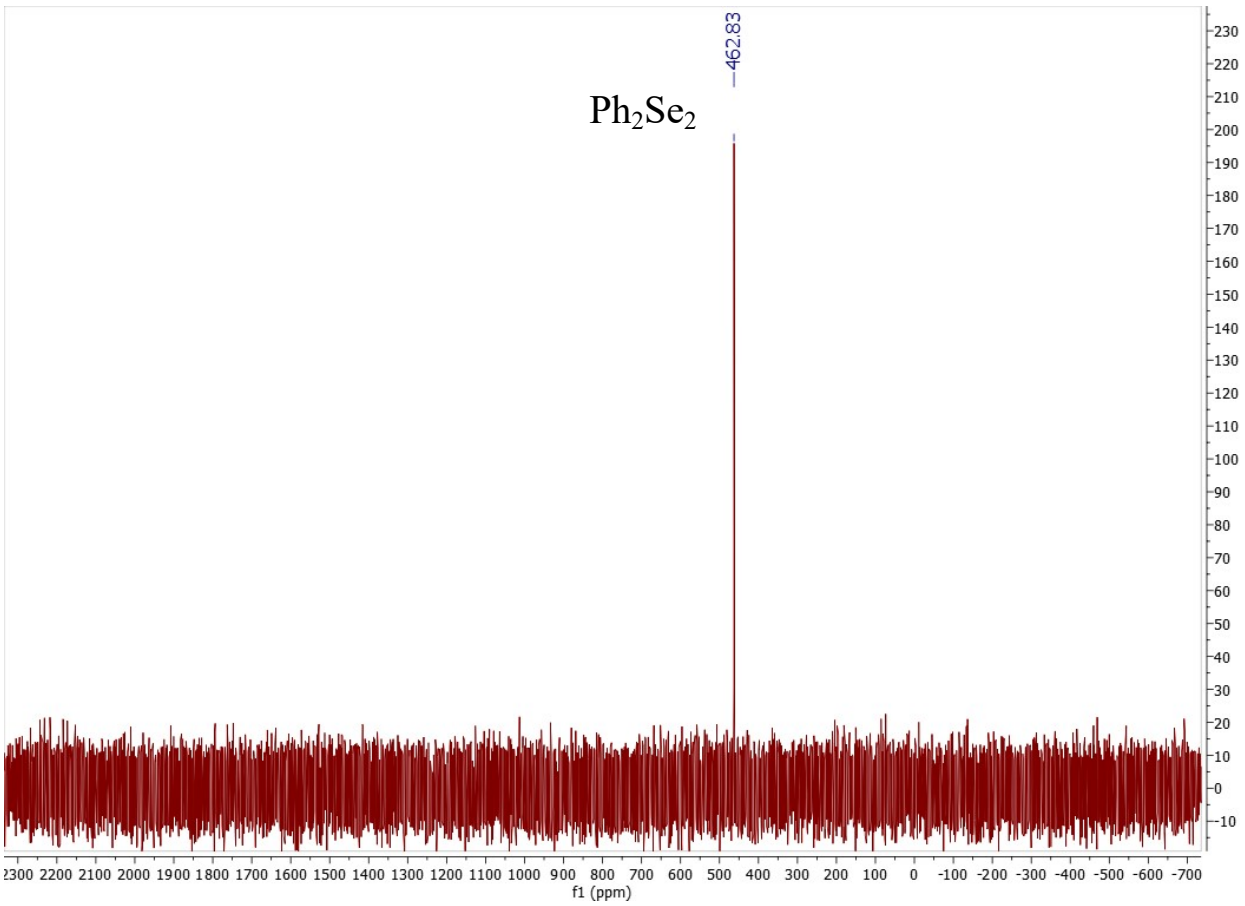

Figure S21. ^{77}Se NMR spectrum of mixture $Tol^{F}_{2}Te$:Ph_2Se_2 in molar ratio 20:1 in $CDCl_3$ at 298 K.